eJSE International
Electronic Journal of Structural Engineering 18(2) 2018

Numerical Simulation of Stretch Bending for L-section Aluminum Alloy Profile

Y. Liu, L. Song, J. Yin, F. Ma, Z. Sha, D. Yang, S. Zhang*
School of Mechanical Engineering, Dalian Jiaotong University, Dalian, China
*E-mail: zsf@djtu.edu.cn

ABSTRACT: High precision stretch bending of aluminum alloy profile is the key technology for making car's frame body. A numerical simulation study on the displacement-controlled process for a typical kind of L-section aluminum alloy profile used in high-speed rail with finite element analysis software is presented. The effect of different friction coefficients, with or without baffle and cover plate on the equivalent stress, strain and cross-sectional distortion are investigated. It is shown that the increase of the friction coefficient can increase the cross-sectional distortion, equivalent stress and strain. The installation of baffle and cover plate can significantly reduce the cross-sectional distortion in the middle section of the profile, and increase the equivalent stress and strain to some extent.

KEYWORD: aluminum alloy; stretch bending; numerical simulation; cross-sectional distortion

1 INTRODUCTION

Because of many advantages such as light weight, high security and easy recycled, aluminum alloy is used widely in the lightweight structure of vehicle. The bent aluminum alloy profile is the main component of high-speed train skeleton, occupies a considerable proportion in contemporary high-speed rail, and it is an important factor to influence the assembly precision and service life of high-speed train. There are many methods for the bending of aluminum alloy, such as compression-bending, roll bending, rotation bending, stretch bending and so on [1]. Compared with others methods, stretch bending has following advantages [2, 3]:

(1) For some complicated structures, it can achieve bend by using different loading methods;

(2) It is conspicuously effective for profiles with high tensile strength ratio;

(3) Because of the impacts of tangential force and post-stretching, the stress inside profile is uniformly distributed, which can obviously improve forming accuracy, quality of surface and reduce springback at the same time;

(4) It has the characteristic of flexible manufacturing.

Aluminum alloy with L-section is mainly used in door column of high-speed train and manufactured by the method of stretch bending. The shape and dimensional accuracy after forming is strictly required to meet the processing standard of the subsequent processing technology. Within the stretch bending process, there are not only some problems which are encountered in the formation of sheet, such as crack, wrinkling and springback, but also special problems such as the cross-sectional distortion and longitudinal distortion [4]. A numerical simulation study on the stretch bending process of the dissymmetry aluminum alloy profile with L-section with finite element analysis software ABAQUS is presented. The effect of different friction coefficients, with or without baffle and cover plate on the equivalent stress, strain and cross-sectional distortion are investigated, which provides helpful guidance to the stretch bending process of aluminum alloy profile.

2 MOVING TRAJECTORY OF CLAMPS IN STRETCH BENDING

2.1 *Profile stretch bending control method*

The process of stretch bending can be controlled by the method of the stretching force and displacement control [5], which are both used in industrial production. The simulation is made by the displacement control method in this paper which is to control the displacement of clamps during the bending process and utilize the moving of clamps to make profile bent [6]. The whole process can be divided into three steps: pre-stretching, bending and post-stretching. Firstly, the profile is applied with a certain amount of pre-tension during the pre-deformation stage before the bending process. Then, the profile is bent through controlling the displacement of clamp in the bending stage. Finally, a certain post-tension is exerted to strengthen the shape of profile. The above process is shown in Figure 1.

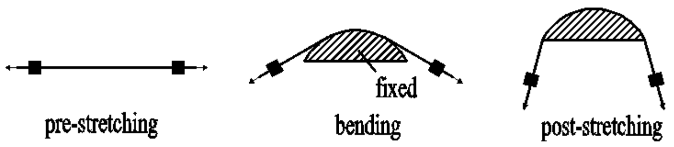

Figure 1. Process of stretch bending forming

2.2 *Moving trajectory of clamps*

Traditionally, "pre-stretching, bending, post-stretching" pattern is chosen. However, during the bending process, There is reverse deformation trend in the rapid deformation area of profile because the pressure on the both sides of profile will be exerted downward and inward when the shaping curvature is too large, which is not beneficial to achieve a better lamination of the profile and die. Therefore, the bending phase in the “pre-stretching, bending, post-stretching” mode is modified to the bending while stretching, which is named as "stretch bending". So, it is convert into the "pre-stretching, stretch bending, post-stretching" mode.

Bring drape forming quantity δ which is artificially given and neglect natural elongation indicator during the stretch bending process. During the bend process, a drape forming quantity in every increment δ_n is given as:

$$\delta_n = \frac{1}{n} \times \delta \tag{1}$$

Where i = the increment step; and n = the total number of the increment steps.

Therefore, the length of profile $L(i)$ is an incremental function with the increment step i as a independent variable when calculating the trajectory of clamp in the stretch bending stage. So, the length of profile $L(i)$ is given as:

$$L(i) = L + \delta_n \times i \tag{2}$$

Where L = the original length of workpiece.

The curvature of workpiece on the right side is constant, a constant curvature trajectory calculation method is used. The principle of the clamp on the right side is shown in Figure 2.

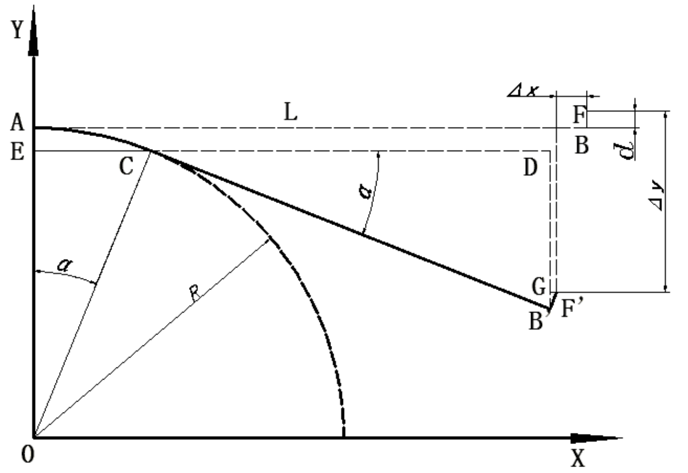

Figure 2. Schematic diagram for constant curvature trajectory design

The increment of each step along the X and Y directions are expressed respectively as:

$$\Delta x = L - \left[R \cdot \sin\alpha_i + \left(L(i) - R \cdot \alpha_i \right) \times \cos\alpha_i + d \cdot \sin\alpha_i \right] \tag{3}$$

$$\Delta y = d + R \times (1 - \cos\alpha_i) + \left(L(i) - R \cdot \alpha_i \right) \times \sin\alpha_i - d \cdot \cos\alpha_i \tag{4}$$

Where L = the length of the profile after pre-stretching; R = the radius of the section’s neutral layer; d = the distance between the point F and the neutral layer of the profile and α = the angle of bending.

The curvature of workpiece on the left side remains unchanged in one area, but the curvature are different in the other area. Therefore, it is necessary to precisely control the stretch bending process of the segmented curvature in order to ensure the smoothness of the profile when calculating the trajectory of clamp, which is beneficial to improve the lamination condition and forming accuracy. The principle of the clamp on the left side is shown in Figure 3.

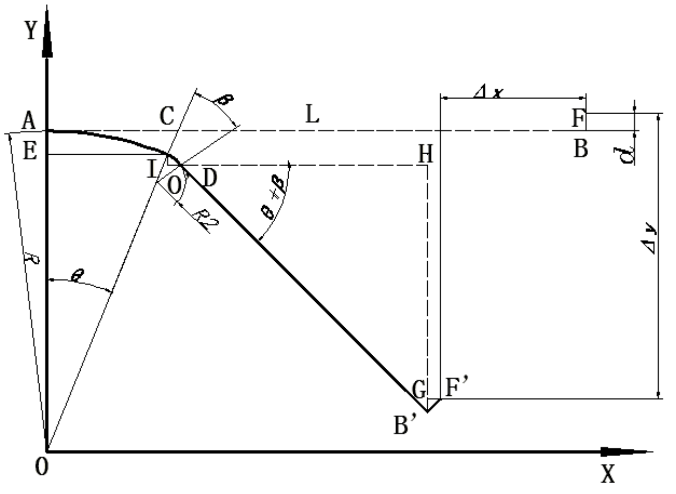

Figure 3. Schematic diagram for sectional curvature trajectory design

The increment of each step along the X and Y directions are expressed respectively as:

$$\Delta x = L - [R_1 \cdot \sin\theta_l + R_2 \cdot \sin(\theta_l + \beta_k) - R_2 \cdot \sin\theta_l + (L(i) - R_1 \cdot \theta_l - R_2 \cdot \beta_k) \times \cos(\theta_l + \beta_k) + d \cdot \sin(\theta_l + \beta_k)] \quad (5)$$

$$\Delta y = d + R_1 \times (1 - \cos\theta_l) + R_2 \times [\cos\theta_l - \cos(\theta_l + \beta_k)] + (L(i) - R_1 \cdot \theta_l - R_2 \cdot \beta_k) \times \sin(\theta_l + \beta_k) - d \cdot \cos(\theta_l + \beta_k) \quad (6)$$

Where R_1 = the bending radius of the first arc; R_2 = the bending radius of the second arc; θ_l = the bending angle of the first arc; and β_k = the bending angle of the second arc.

3 MATERIAL MODEL OF THE PROFILE

According to the flow and hardening law of aluminum alloy material, the stress-strain relationship of aluminum alloy can be described by Krupkowsky formula [7]:

$$\sigma = K(\varepsilon_p + \varepsilon_o)^n, \ \varepsilon_o = \sqrt[n]{\frac{\sigma_s}{K}} \quad (7)$$

Where σ = the real stress; ε_p = the plastic strain; ε_o = the initial plastic strain; K = the hardening coefficient; σ_s = the ultimate yield stress; and n = the strain strength coefficient.

The material of profile is Al6005-T4, which belongs to the aluminum alloy of Al-Mg-Si series, with the advantages of moderate strength, good squeezing and corrosive resistance. After T4 heat treatment, Al6005-T4 has good plastic deformation ability [8, 9]. The material property parameters are shown in Table 1.

Table 1. The material performance parameters of Al6005-T4

ρ	E	μ	σ_s	K
g/cm³	Gpa		Mpa	Mpa
2.6	70	0.3	139	401.5

4 FINITE ELEMENT MODEL OF STRETCH BENDING

In the numerical simulation process, the discrete model of the machining technology should be established firstly. The accuracy of the model are directly related to the accuracy of the finite element analysis results [10]. The trajectory of clamps, material physical, mechanical characteristics and boundary conditions according to the actual process of stretch bending need to be set in the finite element model of stretch bending, what's more the appropriate contact algorithm for calculation should be selected.

The pre-stretching amount is 1%, the stretching amount is 4.5% and the post-stretching amount is 0.5% [11].The length of workpiece is about 3400 mm and the width of the web is 6 mm. After the stretch bending, the contour is composed of the three arcs and straight line segment, which is asymmetric in portrait. As it can be seen from Figure 4.

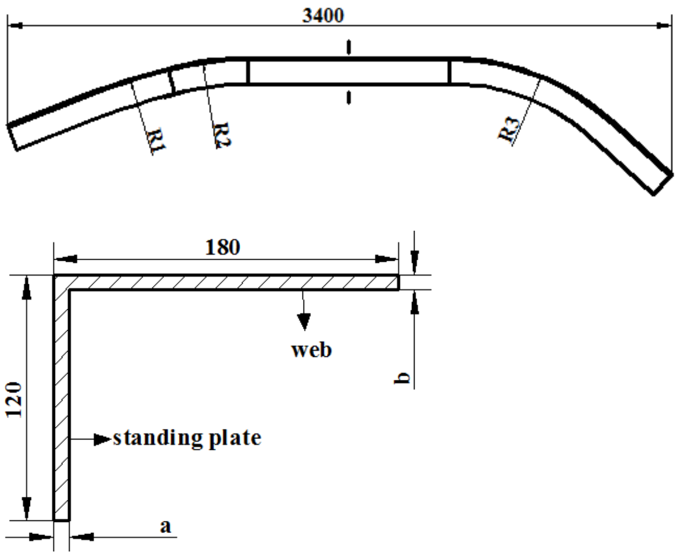

Figure 4. L-section workpiece geometry

Commercial finite element software ABAQUS is chosen to conduct simulations for stretch bending process, which have an explicit dynamic code, the explicit dynamic algorithm has proven valuable in solving profile forming [12]. In the finite element model, the deformation of the die and clamps are smaller than the deformation of workpiece. For the sake of saving time, the clamps and die are set into the discrete rigid body, the clamps are simplified rectangle thin plates and bounded to profile in the constraint setting, so that the motion of the clamps drive the bending of workpiece. Considering the stress of the thickness direction have a certain influence on simulation precision due to the web and the standing plate are not the same in thickness, so the finite element analysis make use of the solid grid unit. The workpiece's cross-sectional distortion can be effectively controlled by the baffle and the cover plate together. In this paper, the finite element analysis with or without baffle and cover plate need to be performed together. The load is applied to the cover plate and the effect of the load on the workpiece is transmitted through the cover plate, we use the cover plate as the research object rather than the load because the value of the load is constant. Therefore, the baffle and cover plate are installed on the basis of the original model, restraint force are applied on the cover plate and a gap of 2 mm is kept between the baffle and the workpiece. Similarly, the baffle and cover plate also adopt the discrete rigid body in order to save the computing time. This model grid type is C3D8R and shown in Figure 5.

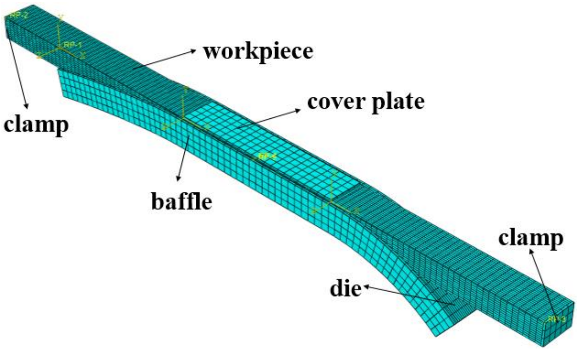

Figure 5. The finite element model

5 NUMERICAL SIMULATION RESULTS

In the process of stretch bending, the change of section's shape is unavoidable, which is called cross-sectional distortion [13]. The reason for the cross-sectional distortion is that units below the neutral section of the profile produce different compressive strain and tensile strain under the joint action of the tangential, longitudinal and radial forces during the stretch bending process. It is known as the cross-sectional distortion of the surface that changes in geometric shapes such as radial thickening, longitudinal shrinkage and axial tension or compression. Because the yield strength of aluminum alloy profiles is much smaller than steel, the standing plate below neutral layer will be compressed. This compressive stress not only leads to the increase of the plate's thickness, but also makes plate unsteadiness, resulting in deformation [14]. The cross-sectional distortion is defined by recording the lateral offset of nodes at the bottom of the standing plate during the stretch bending process. The cross-sectional distortion (n_1) is given as:

$$n_1 = \frac{\Delta x}{d} \tag{8}$$

Where Δx = the lateral offset; and d = the width of the baffle.

5.1 *The effect of friction coefficient on forming accuracy*

5.1.1 *The effect of friction coefficient on equivalent stress and strain*

The node path was created in the middle of the web, and the equivalent stress and strain distribution of the web were obtained with friction coefficients of 0.1, 0.2, 0.3, 0.4, and 0.5, as shown in Figure 6.

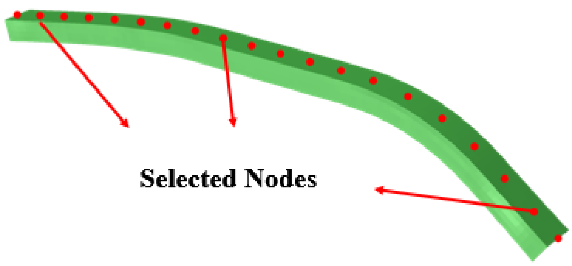

Figure 6. The node path of the web

The curves of stimulation results in Figure 7 and Figure 8 are drawn respectively. The X coordinate of each node is the horizontal axis, the equivalent stress S,Mises and the equivalent strain PEEQ are the vertical axis respectively.

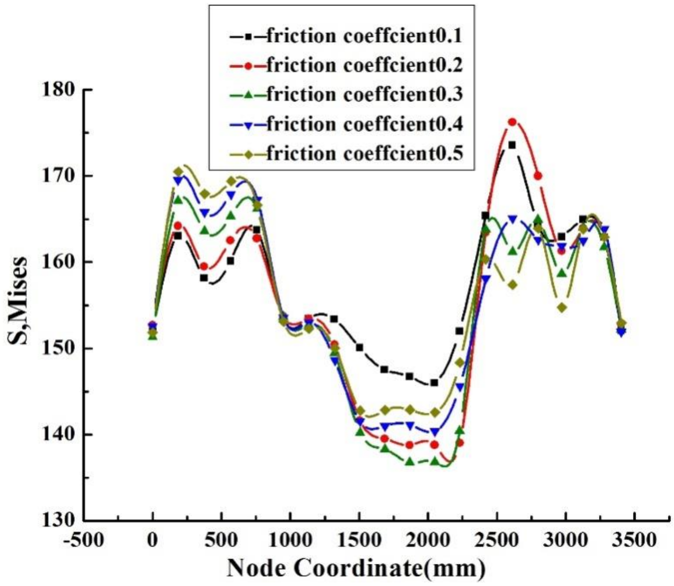

Figure 7. The comparison of the web's equivalent stress with different friction coefficients

From Figure 7, due to the curvature of the profile on both sides and two bend angles on the left side, the equivalent stress on both sides is larger than that in the middle and there are two fluctuations on the left side. The equivalent stress in the left deformed area increases gradually, in the middle decreases first, and then increases, and in the right deformation area decreases when the friction coefficient increases from 0.1 to 0.5. And the equivalent stress differences between the left and middle deformed areas increase. The overall stress distribution of the profile is uniform. The equivalent strain of the web with different friction coefficients are shown in Figure 9.

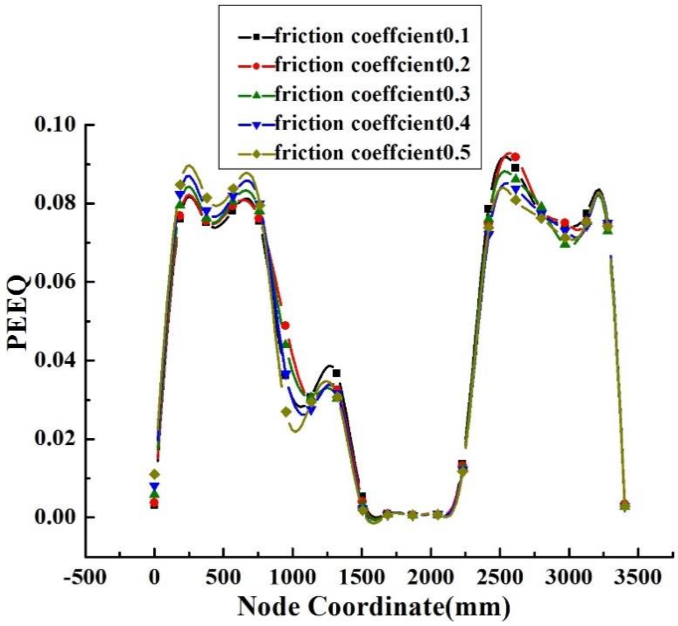

Figure 8. The comparison of the web's equivalent strain with different friction coefficients

It can be seen from Figure 8 that due to the curvature of the profile on the both sides and the two bend angles on left side, the equivalent strain on both sides is larger than that in the middle and there are two fluctuations on the left side. The overall trend are similar to the equivalent stress. When the friction coefficient increases from 0.1 to 0.5, the equivalent strain in the left deformation area gradually increase, the equivalent strain decreases in the right deformed area. And the equivalent strain in the middle is extremely small, volatility can be neglected.

With the increase of the friction coefficient, the tensile stress and the friction between the workpiece and the die increase during the process of stretch bending. This leads to the increase of the unit yield stress and the plastic strain. Because the bending radius of workpiece on the left side is smaller than that on the right side, workpiece on the left side makes contact with the die earlier, the friction has more regular influence in the left and middle areas. When the bending on the left side is completed, the frictional force plays a major role on the left side, so the equivalent stress gradually increases and then the bending force plays a major role in the bending process on the right side. The bending force is weakened with the increase of the friction coefficient, the equivalent stress is reduced.

5.1.2 *The effect of friction coefficient on cross-sectional distortion*

The node path was created at the bottom of the standing plate and the cross-sectional distortion of the standing plate was measured respectively under different positions with friction coefficients of 0.1, 0.2, 0.3, 0.4, and 0.5, as shown in Figure 9.

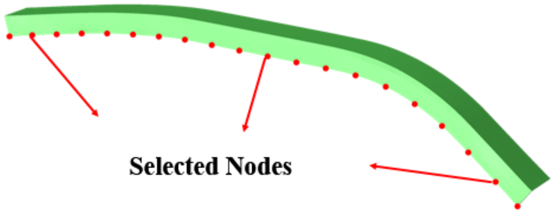

Figure 9. The node path of the standing plate

The curves are drawn in Figure 10. The X coordinate of each node is the horizontal axis, the cross-sectional distortion (n_1) is the vertical axis.

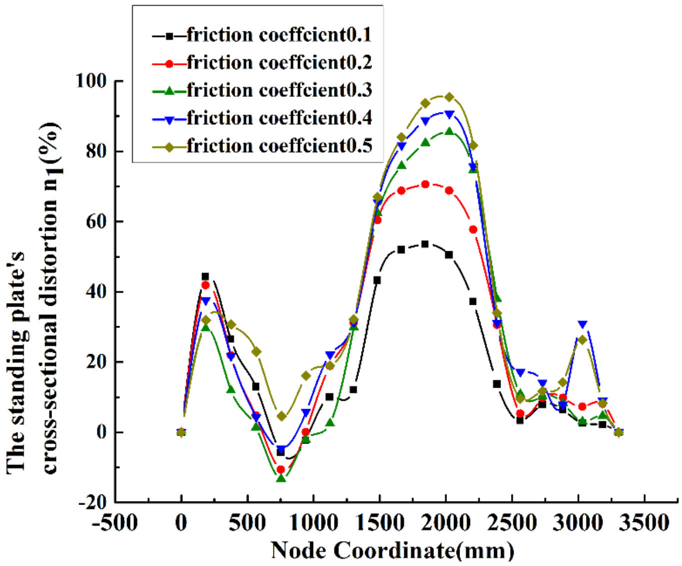

Figure 10. The comparison of the standing plate's cross-sectional distortion with different friction coefficients

By observing the Figure 10, because the two sides of the profile are bent and the standing plate shrink to the middle, leading to the standing plate in the middle are pressed and in the corners are pressed inward, so the cross-sectional distortion in the middle is larger than the two sides. There are two fluctuations in the left area and the cross-sectional distortion in the left area is slightly larger than the right side. The maximum deformation of the standing plate rise gradually from 53.6% to 95.4% as the friction coefficient increases from 0.1 to 0.5.

From the simulation results, it can be seen that the friction increases between the two sides of workpiece and the die, so that the inward compressive stress of the standing plate decrease on the both sides of workpiece, so the inward dimple decrease with the increase of the friction coefficient. The outward compressive stress of workpiece in the middle become large, so does the outside asperities, resulting in cross-sectional distortion of the standing plate's middle part increase.

5.2 *The effect of the baffle and cover plate on forming accuracy*

The baffle is mounted on the workpiece's standing plate, the cover plate is mounted on the workpiece's web. In actual working conditions, the baffle and the cover plate are applied on the workpiece together. Their influence on the workpiece is a joint effect result. So we combine them to analyze the effect on the cross-sectional distortion.

5.2.1 *The effect of the baffle and cover plate on equivalent stress and strain*

Both the baffle and the cover plate can suppress the cross-sectional distortion. The cross-section distortion is mainly investigated in the paper, so we combine the baffle and the cover plate for analysis. When the friction coefficients are 0.1, 0.3 and 0.5, the equivalent stress of the web is simulated with the baffle and cover plate, and the simulation results are shown in Figure 11.

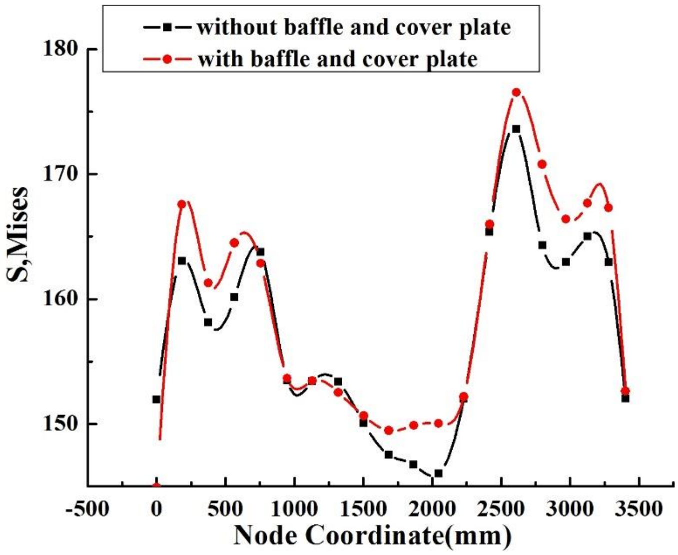

Figure 11a. The friction coefficient is 0.1

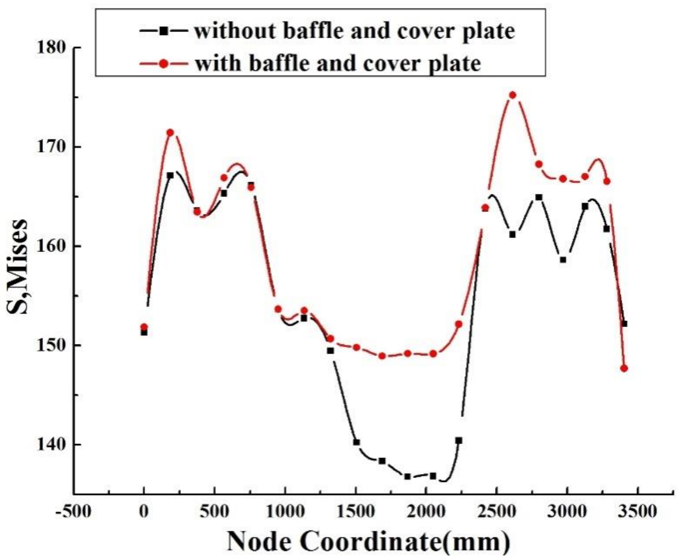

Figure 11b. The friction coefficient is 0.3

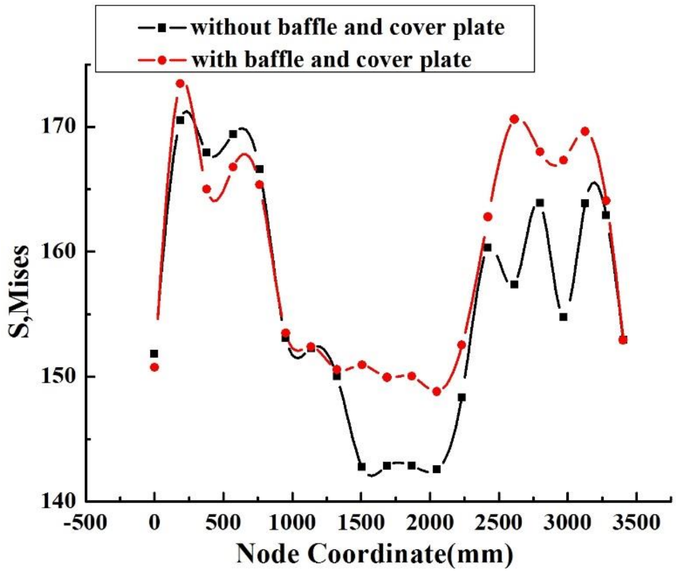

Figure 11c. The friction coefficient is 0.5

Figure 11. The comparison of the web's equivalent stress with or without baffle and cover plate

Figure 11 shows that after installing the baffle and cover plate, the maximum equivalent stress of workpiece increases from 1.73×10^2 Mpa to 1.77×10^2 Mpa when the friction coefficient is 0.1 and the maximum equivalent stress increases from 1.70×10^2 Mpa to 1.74×10^2 Mpa when the friction coefficient is 0.5, the increases amplitude reach 2.3% and 2.4% respectively. The distribution of the equivalent stress in the middle is uniform, and the holistic equivalent stress becomes large. The deformation of workpiece is constrained by the baffle plate and the effect of the force exerted by the cover plate on workpiece, which bring about the increase of the compressive stress and the tensile stress of workpiece. Therefore, the equivalent stress increases by a certain extent. The equivalent strain of the web is simulated with baffle and the cover plate, and the simulation results are shown in Figure 12.

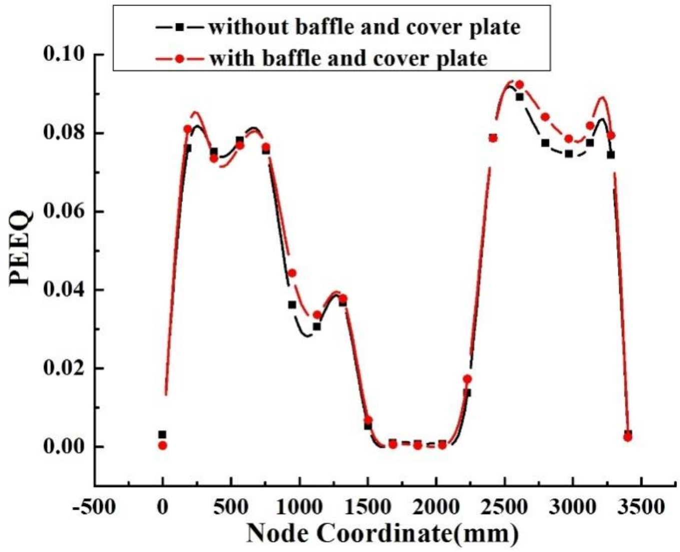

Figure 12a. The friction coefficient is 0.1

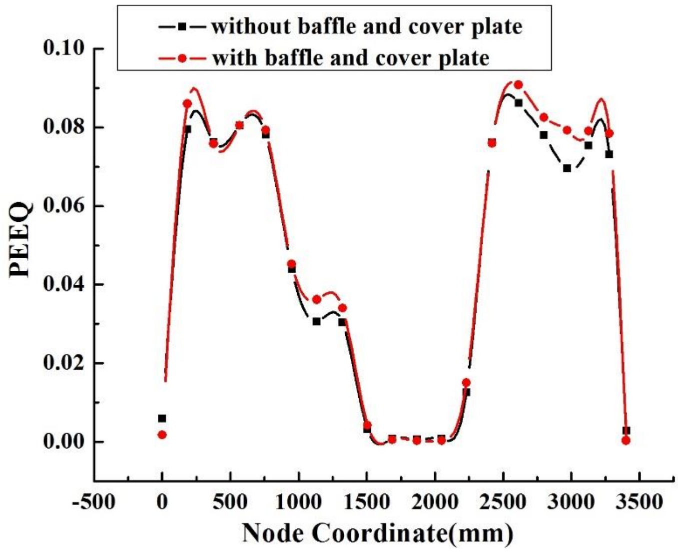

Figure 12b. The friction coefficient is 0.3

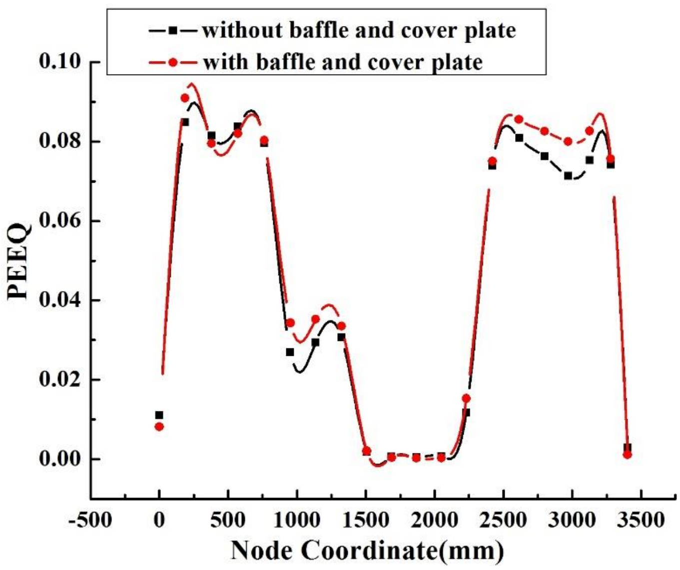

Figure 12c. The friction coefficient is 0.5

Figure 12. The comparison of the web's equivalent strain with or without baffle and cover plate

Figure 12 show that after installing the baffle and cover plate, the maximum equivalent strain of workpiece increase from 8.9×10^{-2} to 9.2×10^{-2} when the friction coefficient is 0.1 and the maximum equivalent strain of workpiece increase from 8.4×10^{-2} to 9.0×10^{-2} when the friction coefficient is 0.5, the increase amplitude reach 3.3% and 7.1% respectively. Compared to the simulation without baffle and cover plate, the equivalent strain in the left deformed area increases, the equivalent strain in the right deformed area increase by a certain degree and the equivalent strain's change in the middle can be neglected.

From the simulation results, it can be observed that the baffle and cover plate restrain the deformation of workpiece. The equivalent stress of profile's element increase and the profile can enter the plastic state earlier due to the compressive stress increase, which bring about the holistic equivalent strain increase.

5.2.2 *The effect of the baffle and cover plate on cross-sectional distortion*

The numerical simulation of stretch bending is carried out to analyze the cross-sectional distortion of profile with or without the baffle and cover plate when the friction coefficient is 0.1, 0.3 and 0.5 respectively, as shown in Figure 13.

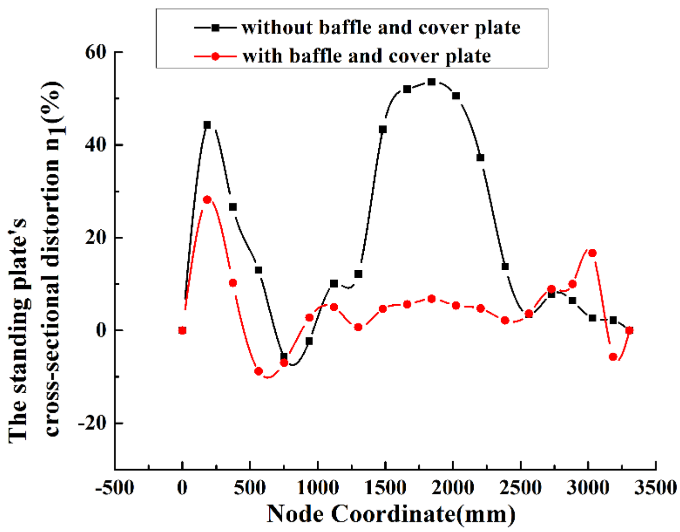

Figure 13a. The friction coefficient is 0.1

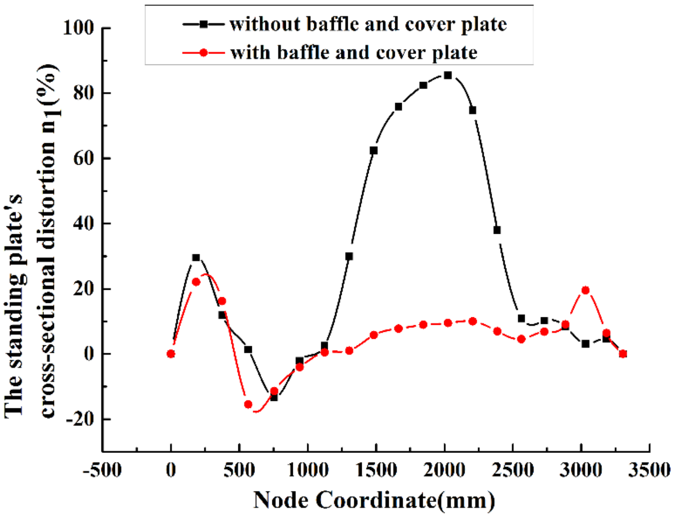

Figure 13b. The friction coefficient is 0.3

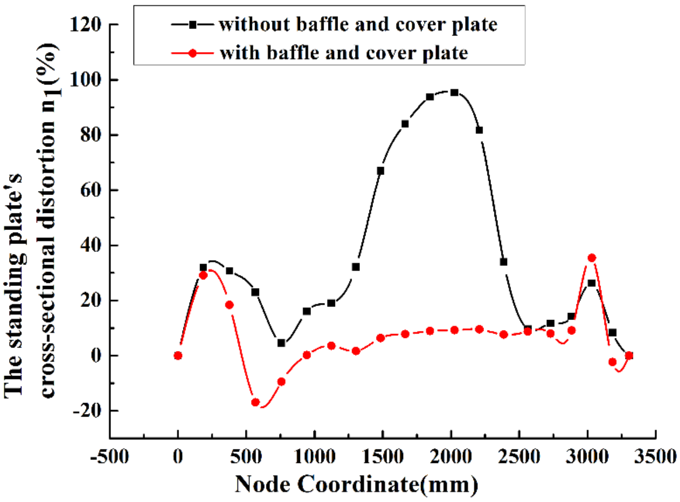

Figure 13c. The friction coefficient is 0.5

Figure 13. The comparison of the standing plate's cross-sectional distortion with or without baffle and cover plate

The data in Figure 13 show that after installing the baffle and cover plate, the cross-sectional distortion in the middle area reduces greatly, and the cross-sectional distortion on the both sides increases. The baffle and cover plate can obviously reduce the cross-sectional distortion in the middle. During the stretch bending process, the baffle and cover plate have prohibitive influence on the outward deformation of the standing plate and the deformation is reduced, which lead to the increase of the inside deformation of workpiece's both sides.

6 COMPARISON OF TEST RESULTS

The bending test of the profile was carried out on the CNC arm-type stretch bending machine produced by ERIR PRESS SYSTEMS. The bending process is controlled by the displacement-controlled. The computer generates program files by setting the clamp path and material mechanical properties to adjust the movement of the stretching cylinder and the rotating arm. The test uses L-shaped aluminum profile and the material is AL6005-T4. The material of die, baffle and cover plate is Q235 (the friction coefficient is about 0.3). The two sides of the workpiece were clamped by the jaws, and restraint forces were applied on the cover plate. The working picture of stretch bending process is shown as Figure 14. The gaps between the baffle and the workpiece were about 5 mm. The test points were taken every 100 mm from the outer edge of 30 mm in the middle of the inside of the formed piece's standing plate, and the flatness error was measured. The points were taken every 100 mm from the outer edge of about 30 mm in the middle of the inside of the simulation result's standing plate after installing the baffle and cover plate when the friction coefficient is 0.3 and the gaps between the baffle plate and the workpiece was 5 mm, and the flatness error was measured from the right side to the left side. The two sets of data are shown in Figure 15.

Figure 14. The working picture of stretch bending process

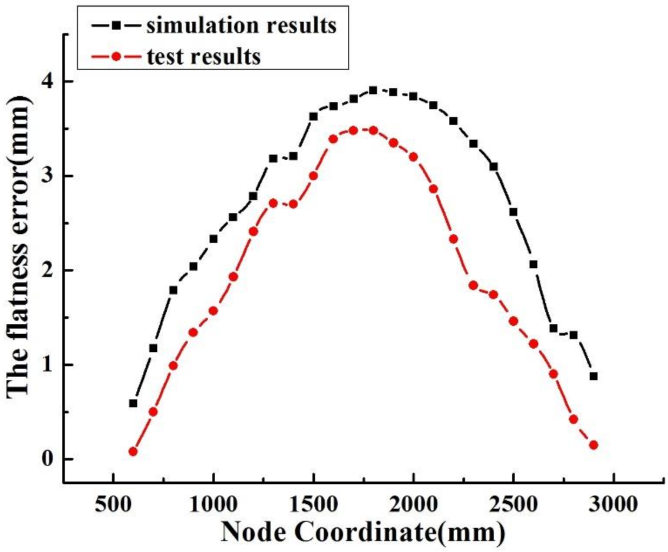

Figure 15. The comparison of the standing plate's flatness error in simulation and experiment

The test data measured with dial test meter, the evaluation datum is the three-point method that the standard flat-plate is selected as the measurement reference, the three points farthest from the measured surface are adjusted to be as high as the standard flat-plate and measured with the micrometer. In simulation results, the selected points' displacement along the cross-sectional direction before and after the simulation are extracted in the post-processing, which are approximately replaced as the flatness error of the simulation results.

By comparing the simulation and test results, the simulation data is slightly larger than the test data. The main reasons are as follows: first, the deformation of the standing plate is reduced along the cross-sectional direction when the loads are removed. The test data is the result of the springback, but the simulation data is the result of the stretch bending, which lead to some errors; second, the flatness error of the simulation results is approximately replaced by the nodes' displacement; third, the settings of the friction coefficient and material properties had differences compared to the actual situation. They all lead to the differences of the flatness error eventually. However, the overall trend of results is similar, there are gradually rising from both sides toward the middle.

7 CONCLUSIONS

In this paper, the stretch bending process of the displacement-controlled profile is numerically simulated for a typical L-section aluminum alloy profile used in high-speed rail by finite element software ABAQUS. The effect law of different friction coefficients and with or without baffle and cover plate on the equivalent stress, strain and the cross-sectional distortion are analyzed, and the conclusions are drawn as follows:

(1) With the increase of the friction coefficient, the equivalent stress and equivalent strain in the left and middle deformation areas of the web increase by a certain extent, and the deformation in the right area decrease a little.

(2) With the increase of the friction coefficient, the cross-sectional distortion is smaller on the both sides where the workpiece is contact with the clamps. However, the cross-sectional distortion in the middle deformation area increase to certain extent.

(3) When the baffle and cover plate are installed, the equivalent stress and equivalent strain increase and the deformation of the workpiece is uniform. The wrinkling phenomenon can be effectively avoided.

(4) When the baffle and cover plate are installed, the cross-sectional distortion in the middle deformation area are effectively reduced, but the cross-sectional distortion on the both sides increase.

8 ACKNOWLEDGMENTS

The authors gratefully acknowledge the financial support of National Natural Science Foundation of China (No. 51475066) and Outstanding Talent Project of Education Department of Liaoning Province (No. LR2015012).

REFERENCES

1. Huang, L., "Aircraft Manufacturing Technology", *Beijing Aviation Industry Press*, 1992.
2. Paulsen, F., and Welo, T., "Application of numerical simulation in the bending of aluminum alloy profiles", *Journal of Materials Processing Technology*, Vol. 58, No. 2, 1996, pp 274-285.
3. Stelson, K., "Modeling and Closed-Loop Control of Stretch Bending of Aluminum Rectangular Tubes", *Journal of Manufacturing Science & Engineering*, Vol. 125, No.1, 2003, pp 113-119.
4. Corona E. "A Simple Analysis for Bend - Stretch Forming of Aluminum Extrusions", *International Journal of Mechanical Sciences*, Vol. 46, No.3, 2004, pp 433-448.
5. Clausen, A. H., Hopperstad, O. S., and Langseth, M., "Sensitivity of Model parameters in stretch bending of aluminium extrusions", *International Journal of Mechanical Sciences*, Vol. 43, No.2, 2001, pp 427-453.
6. LIU X Z, ZHANG S L, LI S T, et al. "Research on stretch bending of hollow aluminum alloy profile", *Forging & Stamping Technology*, Vol. 40, No.5, 2015, pp 69-73.
7. Lu, R., "Study on Stretch bending Forming Simulation and Accuracy Control of Profiles", *Jilin University*, 2014.
8. Rometsch, P. A., Zhang, Y., and Knight, S., "Heat treatment of 7xxx series aluminium alloys - Some recent development", *Transactions of Nonferrous Metals Society of China*, Vol. 24, No.7, 2014, pp 2003-2017.
9. Zhang, G., "Effect of Heat Treatment Process on Microstructure and Properties of New Type 6XXX Aluminum Alloy", *Central South University*, 2010.
10. Diao, K., "Stretch bending of aluminum extrusion", Journal of *Beijing University of Aeronautics & Astronautics*, Vol. 31, No. 2, 2005, pp 134-137.
11. Hao T T, Chen M H, Li S L, et al. "Research on Stretch Bending Process for Asymmetric Cross-section Extrusions", *Machinery Manufacturing*, Vol. 52, No.6, 2014, pp 40-42.
12. Wang S H, Cai Z Y, Li M Z, et al. "Numerical simulation on the local stress and local deformation in multi-point stretch forming process", *International Journal of Advanced Manufacturing Technology*, Vol. 60, No.9, 2012, pp 901-911.
13. Li, X. Q., Li, H., and Li, D. S., "Springback Simulation in Stretch Bending of Aluminum Extrusions Using Static Implicit and Dynamic Explicit FE Codes", *Advanced Materials Research*, 2011, pp 295-297, 1606-1612.
14. Chen, M. H., Gao. L., and Mao, H. H., "Numerical Simulation of Stretch Bending Process and Springback for T Section Aluminum Extrusions", *Key Engineering Materials*, 2006, pp 315-316, 416-420.